Frost, Ray L. and Cejka, Jiri and Keeffe, Eloise C. and Sejkora, Jiri (2009) *Raman spectroscopic study of the mixed anion sulphate-arsenate mineral parnauite Cu9[(OH)10|SO4|(AsO4)2].7H2O*. Journal of Raman Spectroscopy, 40(11). pp. 1546-1550.

Raman spectroscopic study of the mixed anion sulphate-arsenate mineral parnauite $Cu_9[(OH)_{10}|SO_4|(AsO_4)_2]\cdot 7H_2O$

Ray L. Frost [1] • Jiří Sejkora, [2] Jiří Čejka [1, 2] and Eloise C. Keeffe [1]

[1] Inorganic Materials Research Program, School of Physical and Chemical Sciences, Queensland University of Technology, GPO Box 2434, Brisbane Queensland 4001, Australia.

[2] National Museum, Václavské náměstí 68, CZ-115 79 Praha 1, Czech Republic.

The mixed anion mineral parnauite $Cu_9[(OH)_{10}|SO_4|(AsO_4)_2]\cdot 7H_2O$ has been studied by Raman spectroscopy. Characteristic bands associated with arsenate, sulphate, hydroxyl units are identified. Broad bands are observed and are resolved into component bands. Two intense bands at 859 and 830 cm^{-1} are assigned to the ν_1 $(AsO_4)^{3-}$ symmetric stretching and ν_3 $(AsO_4)^{3-}$ antisymmetric stretching modes. The comparatively sharp band at 976 cm^{-1} is assigned to the ν_1 $(SO_4)^{2-}$ symmetric stretching mode and a broad spectral profile centered upon 1097 cm^{-1} is attributed to the ν_3 $(SO_4)^{2-}$ antisymmetric stretching mode. A comparison of the Raman spectra is made with other arsenate bearing minerals such as carminite, clinotyrolite, kankite, tilasite and pharmacosiderite.

KEYWORDS: parnauite, strashimirite, arsenate minerals, Raman spectroscopy, sulphate, hydroxyl, molecular water

• Author to whom correspondence should be addressed (r.frost@qut.edu.au)

INTRODUCTION

Parnauite $Cu_9(AsO_4)_2(SO_4)(OH)_{10}\cdot 7H_2O$ is an uncommon mixed anion mineral containing both sulphate and arsenate [1-3] .The mineral is probably orthorhombic with point group 2/*m* 2/*m* 2/*m* [4]. Sometimes the mineral is found with other minerals such as leogangite, goudeyite and strashimirite. Another similar formulated mineral is leogangite $Cu_{10}(AsO_4)_4(SO_4)(OH)_6\cdot 8H_2O$. Other minerals containing sulphate and arsenate with the copper cation are arsentsumebite, arthurite, chalcophyllite, clinotyrolite, gatrellite and thometzekite.

Parnauite is formed as one of supergene product of weathering of primary copper minerals (chalcopyrite, tennantite). Originally, it was found at Majuba Hill Mine, Pershing County, Nevada (U.S.A), in association with chrysocolla and other supergene minerals [3]. Parnauite was found later also on many further localities, however, always as a very rare mineral species [4]. No X-ray single crystal structure data are as yet available. Chemical composition of parnauite has been open, because some authors assume that this mineral may contain various content of carbonate ions [1,3]. The studied parnauite was found at the Svätodušná deposit, Lubietová (Slovak Republic) in association with euchroite, olivenite, cornwallite and cornubite.

This research forms part of a comprehensive study of the molecular structure of secondary minerals containing oxy-anions, including uranyl minerals [5-14], formed in the oxide zone, using Raman and infrared spectroscopy. [15-20] To the best of the authors knowledge the Raman (or infrared) spectrum of the mixed anion mineral parnauite has not been published. Further the exact structure of the mineral is not known. Raman spectroscopy is a very powerful technique for the determination of molecular structure of minerals when the exact structure from X-ray diffraction is unknown or uncertain. The objective of this research is to report the Raman properties of parnauite from the Slovak Republic and relate the Raman spectra to the structure of the mineral.

EXPERIMENTAL

Minerals

The studied sample of the mineral parnauite was found at the Svätodušná deposit, the Lubietová ore district, central Slovakia, Slovak Republic, and is deposited in the mineralogical collections of the National Museum Prague. The sample was analysed for phase purity by X-ray powder diffraction and no minor significant impurities were found. Its refined unit-cell parameters for orthorhombic space group $P2_122$, *a* 14.915(7), *b* 14.190(5), *c* 6.003(4) Å, *V* 1270.5(9) $Å^3$, are comparable with the data published for this mineral phase [3]. The mineral was analysed by electron microprobe (Cameca SX100, WD mode) for chemical composition. The results (mean of 14 point analyses) are CaO 0.03, FeO 0.04, CuO 58.04, NiO 0.03, ZnO 0.07, Al_2O_3 0.58, SiO_2 0.26, As_2O_5 16.57, P_2O_5 1.71. Sb_2O_5 1.13, SO_3 4.82, Cl 0.02, H_2O 17.72, sum 101.02 wt. %. The water content was calculated on the basis of charge balance and theoretical content H_2O = 7 pfu. The resulting empirical formula on the basis of (As+P+S+Sb+Si) = 3 apfu is $[Cu_{9.12}Al_{0.14}Zn_{0.01}]_{\Sigma 9.27}[(AsO_4)_{1.80}(PO_4)_{0.30}]_{\Sigma 2.10}[(SO_4)_{0.75}(SbO_3OH)_{0.09}(SiO_4)_{0.05}]_{\Sigma 0.89}[(OH)_{10.51}Cl_{0.01}]_{\Sigma 10.52}$. $7H_2O$. No carbonate was detected in the analyses. The compositions of this minerals has been reported by Anthony *et al.* (page 442) [4].

Raman spectroscopy

The crystals of parnauite were placed and oriented on the stage of an Olympus BHSM microscope, equipped with 10x and 50x objectives and part of a Renishaw 1000 Raman microscope system, which also includes a monochromator, a filter system and a Charge Coupled Device (CCD). Raman spectra were excited by a HeNe laser (633 nm) at a resolution of 2 cm^{-1} in the range between 100 and 4000 cm^{-1}. Details of the experimental procedure have been published. [5-14]

Spectral manipulation such as baseline adjustment, smoothing and normalisation were performed using the Spectracalc software package GRAMS (Galactic Industries Corporation, NH, USA). Band component analysis was undertaken using the Jandel 'Peakfit' software package which enabled the type of fitting function to be selected and allows specific parameters to be fixed or varied accordingly. Band fitting was done using a Lorentz-Gauss cross-product function with the minimum number of component bands used for the fitting process. The Gauss-Lorentz ratio was maintained at values greater than 0.7 and fitting was undertaken until reproducible results were obtained with squared correlations of r^2 greater than 0.995.

RESULTS AND DISCUSSION

Raman spectroscopy of the arsenate anion

The arsenate ion, $(AsO_4)^{3-}$, is a tetrahedral unit with T_d symmetry and exhibit four fundamental vibrations: the symmetric stretching vibration ν_1 (A_1) (818 cm^{-1}), the doubly degenerate bending vibration ν_2 (E) (350 cm^{-1}), the triply degenerate antisymmetric stretching vibration ν_3 (F_2) (786 cm^{-1}), and the triply degenerate bending vibration ν_4 (F_2) (398 cm^{-1}). The F_2 modes are Raman and infrared active, whereas A_1 and E modes are Raman active only. According to Frost *et al.* the ν_1 $(AsO_4)^{3-}$ vibration may coincide with the ν_3 $(AsO_4)^{3-}$ vibration. It should be noted that the wavenumber of the ν_1 $(AsO_4)^{3-}$ may be greater than that of the ν_3 $(AsO_4)^{3-}$ which is an inversion of the normal behavior shown by most tetrahedral ions, although such an inversion is not unique [21,22]. According to Myneni *et al.* [23], the Td symmetry of $(AsO_4)^{3-}$ unit is rarely preserved in minerals and synthetic compounds, because of its strong affinity to protonate, hydrate, and complex with metal ions. Such chemical interactions reduce $(AsO_4)^{3-}$ tetrahedral symmetry to either C_{3v}/C_3 (corner sharing), C_{2v}/C_2 (edge-sharing, bidentate binuclear), or C_1/C_s (corner sharing, edge-sharing, bidentate binuclear, multidentate]. This symmetry lowering is connected with activation of all vibrations in infrared and Raman spectra and splitting of doubly and triply degenerate vibrations. Nine normal modes may be Raman and infrared active in the case of the lowest C_s symmetry [24].

In aqueous systems, the sulphate anion is of T_d symmetry and has symmetric stretching mode (ν_1) at 981 cm^{-1}, the antisymmetric stretching mode (ν_3) at 1104 cm^{-1}, the symmetric bending mode (ν_2) at 451 cm^{-1} and the ν_4 mode at 613 cm^{-1} [25,26]. The Raman spectrum of the mineral chalcanthite shows a single symmetric stretching mode at 984.7 cm^{-1}. Two ν_2 modes are observed at 463 and 445 cm^{-1} and three ν_3 modes at 1173, 1146 and 1100 cm^{-1}. The ν_4 mode is observed as a single band at 610 cm^{-1}.

Raman spectroscopy of parnauite

The mineral parnauite contains four vibrational spectroscopically distinct units, namely arsenate, sulphate and hydroxyl units as well as water. The mineral is a mixed anion mineral and is one of a number of mixed anion minerals including minerals of the tsumcorite group and minerals such as peisleyite and strashimirite. Mixed anion minerals are more common than might be expected. Isomorphous substitution for arsenate by other anions such as sulphate results in the mineral parnauite.

The Raman spectrum of parnauite in the 700 to 1300 cm^{-1} region is displayed in Fig. 1. This region includes the symmetric stretching region of both the $(AsO_4)^{3-}$ units and the $(SO_4)^{2-}$ ions. A broad envelope of overlapping bands centered upon 835 cm^{-1} is observed. Band component analysis enables bands to be resolved with two intense bands at 859 and 830 cm^{-1} observed. These bands are assigned to the ν_1 $(AsO_4)^{3-}$ symmetric stretching and ν_3 $(AsO_4)^{3-}$ antisymmetric stretching modes. Another band is found at 798 cm^{-1} which may also be ascribed to the ν_3 $(AsO_4)^{3-}$ antisymmetric stretching mode. The observation of multiple bands is attributed to the symmetry reduction of the $(AsO_4)^{3-}$ anion as described above.

A comparison may be made with other arsenate bearing minerals such as carminite, clinotyrolite, kankite, tilasite and pharmacosiderite. [27-30] For carminite bands are observed in the $(AsO_4)^{3-}$ stretching region at 849, 835, 822 and 738 cm^{-1}. The first band is the most intense and is assigned to the ν_1 symmetric stretching mode. The next two bands are assigned to the ν_3 antisymmetric stretching modes. The band at 738 cm^{-1} may be attributed to the hydroxyl deformation mode. For the mineral kankite broad bands are observed at 883 carminite, 832 [ν_1 (A_1)] and 808 cm^{-1}. Component bands are also observed at 790 and 733 cm^{-1}. The latter two bands may be assigned to hydroxyl deformation modes. The Raman spectrum of pharmacosiderite shows two intense bands at 880 and 862 cm^{-1}, attributed to the [ν_3 (F_2)]and 832 [ν_1 (A_1)] vibrational modes. The band at 789 cm^{-1} may be assigned to the OH deformation vibration. For clinotyrolite $(AsO_4)^{3-}$ stretching bands are observed at 841 and 802 cm^{-1}. For picropharmacolite, only broad bands re observed centred upon 866 and 750 cm^{-1}. Talmessite shows well defined Raman bands at 877 and 836 cm^{-1} whereas tilasite displays only a broad band at 820 cm^{-1}.

A further comparison may be made with other arsenate bearing minerals. [31-33] In the Raman spectrum of strashimirite, a broad intense band centred at 845 cm^{-1} is observed and may be band component analysed into component bands at 839 and 856 cm^{-1} which are assigned to the ν_1 $(AsO_4)^{3-}$ symmetric and ν_3 antisymmetric stretching modes. Low intensity bands are also observed at 893 and 975 cm^{-1}. The latter may be attributed to some phosphate substitution. Bands are observed at 826, 843, 891 and 988 cm^{-1}. The two bands at 826 and 843 cm^{-1} are assigned to the ν_1 $(AsO_4)^{3-}$ symmetric and ν_3 antisymmetric stretching modes. Olivenite shows two bands at 826 and 843 cm^{-1} are assigned to the ν_1 $(AsO_4)^{3-}$ symmetric and ν_3 antisymmetric stretching modes. Olivenite shows two bands at 853 and 820 cm^{-1}; Cornwallite at 859 and 806 cm^{-1}, cornubite at 815 and 780 cm^{-1} and clinoclase at 823 and 771 cm^{-1}. By scale expansion of the Y-axis for olivenite, additional very weak bands are observed at 880 and 790 cm^{-1}. The most intense band is assigned to the $\nu_1(A_1)$ symmetric stretching vibration. This assignment differs from that described by Sumin de Portilla [34]. In this work, the $\nu_3(F_2)$ mode was described as splitting into four components at 870, 830, 800 and 750 cm^{-1}. Farmer suggested that the ν_1 and ν_3 modes overlapped and were to be found at the same wavenumber [35]. Whilst this is highly unusual, we suggest that the two vibrations at 853 and 820 cm^{-1} are the $(AsO_4)^{3-}$ symmetric and antisymmetric stretching vibrations respectively. Griffith reported the Raman spectrum of olivenite [36]. Raman bands were found at 880 (A^1), 856 (B_{2u}), 810 (A^1) and 790 (B_{2u}) cm^{-1}. The observation of the bands 853 and 820 cm^{-1} is in good agreement with the data published by Griffith. Bands at 880 and 790 cm^{-1} are in excellent agreement with the data of Griffith. The most intense bands in the Raman spectra are the bands at 853 and 810 cm^{-1}. Factor group analysis suggests that there should be one active Raman band and one active infrared band in this region. The two vibrations result from a loss of site symmetry. The difference in intensity is related to the number of $(AsO_4)^{3-}$ units involved in this site symmetry reduction. Thus the other two infrared bands observed at 800 and 750 cm^{-1} for olivenite are the corresponding ν_3 vibrations. The second band observed at 806 and 771 cm^{-1} is more intense for cornwallite and clinoclase. The $(AsO_4)^{3-}$ stretching vibration for olivenite and cornwallite are in similar band positions, suggesting a similar molecular structure. For cornubite two bands are observed at 815 and 780 cm^{-1}.

The comparatively sharp band at 976 cm^{-1} is assigned to the ν_1 $(SO_4)^{2-}$ symmetric stretching mode. A broad spectral profile centre upon 1097 cm^{-1} may contain the ν_3 $(SO_4)^{2-}$ antisymmetric stretching mode. However the intensity of the band is far too high to be attributed to the sulphate band only. The bands may also include a water librational mode. The intensity of such a band in the Raman spectrum would be expected to be significant although also low in intensity. These bands, however, may also coincide with the $(PO_4)^{3-}$ stretching vibrations. $(PO_4)^{3-}$ anions partly isomorphically substitute $(AsO_4)^{3-}$ anions in the structure of parnauite.

The 300 to 700 cm^{-1} spectral region of parnauite is shown in Fig. 2. The broad spectral profile may be resolved into component bands which are observed at 392, 501, 552 and 615 cm^{-1}. It is likely that the band at 392 cm^{-1} is due to the $(AsO_4)^{3-}$ ν_2 (E) bending mode. It is probable that the two bands at 501 and 615 cm^{-1} are attributable to the symmetric bending mode (ν_2) and the ν_4 modes. The low wavenumber region of parnauite is shown in Fig. 3. A comparison may be made with other arsenate bearing minerals. The bands in the 400 to 500 cm^{-1} region are assignable to the bending ν_4 (F_2) mode. The most intense band is observed at 497 cm^{-1} with other bands at 543 and 467 cm^{-1}. The observation of multiple bands is characteristic of reduced symmetry of the AsO_4 unit in the crystal. The Raman spectra of kankite in this region show an intense band at 492 cm^{-1} and similarly pharmacosiderite shows an intense band at 475 cm^{-1}. For clinotyrolite, an intense band is observed at 493 cm^{-1} with shoulders at 462 and 505 cm^{-1}. The Raman spectrum of picropharmacolite seems ill-defined in this region. In contrast the two minerals tilasite and talmessite have well defined spectra. Talmessite shows two bands at 455 and 445 cm^{-1}. Tilasite shows a sharp band at 410 cm^{-1} with a low intensity band at 493 cm^{-1}. The ν_2 bending mode is normally found at around 349 cm^{-1}. The Fe bearing arsenates of carminite, kankite and pharmacosiderite display a complex set of bands. For carminite bands are observed at 324 and 350 cm^{-1} and are assigned to the ν_2 in-plane bending mode. Strong bands are observed at 210 and 259 cm^{-1} and one possibility for their designation is FeO stretching vibrations. The ν_2 bands for kankite are observed at 398 and 373 cm^{-1} and for pharmacosiderite at 395 and 302 cm^{-1}. These later bands are of comparatively low intensity. For the mineral clinotyrolite, bands in this region are observed at 385, 359 and 314 cm^{-1}. The bands for picropharmacolite are ill defined. For talmessite, strong bands are observed at 363 and 357 cm^{-1}.

The Raman spectrum in the 1300 to 3700 cm^{-1} region is reported in Fig. 4. Three bands which are attributed to OH stretching vibrations are observed at 3348, 3494 and 3566 cm^{-1}. The sharp band at 3566 cm^{-1} is assigned to the OH stretching vibration of the hydroxyl units. The two bands at 3348 and 3494 cm^{-1} are assigned to water stretching modes. Hydrogen plays an extremely important role in the structure and chemistry of oxysalt minerals such as for mixed arsenate sulphates including parnauite and peisleyite [37]. The presence of water adds to the stability of the oxysalt. [38] For any crystal structure the structural unit may be defined as the strongly bonded part of the unit. Structural units are linked together by interstitial species such as univalent and divalent cations and by water groups that are involved in much weaker bonding.

Studies have shown a strong correlation between OH stretching frequencies and both the O···O bond distances and the H···O hydrogen bond distances [39-42]. The elegant work of Libowitzky [43] showed that a regression function can be employed relating the above correlations with regression coefficients better than 0.96 [43]. The function is $\nu_1 = (3592 - 304) \times 109^{\frac{-d(O-O)}{0.1321}}$ cm^{-1}. Two types of OH units are identified in the structure and the known hydrogen bond distances used to predict the hydroxyl stretching frequencies. Thus if we calculate the hydrogen bond distances using the Libowitzky type formula, the 3566 cm^{-1} band provide a hydrogen bond distance of 3.062(5) Å, 3348 cm^{-1} gives 2.766(5) Å, 3494 cm^{-1} gives 2.794(1) Å. The spectrum of parnauite may be divided into two groups of OH stretching wavenumbers: namely 3500–3700 cm^{-1} and 2900–3500 cm^{-1}. This distinction suggests that the strength of the hydrogen bonds as measured by the hydrogen bond distances can also be divided into two groups. An arbitrary cut-off point may be 2.74 Å based upon the wavenumber 3300 cm^{-1}. The hydrogen bond distances 3.062(5) Å may be described as weak hydrogen bonding and the bond distances of 2.766(5) and 2.794(1) Å as slightly stronger hydrogen bonds. Thus by using the position of the bands in the Raman spectrum, an estimate of the hydrogen bond distances can be made. Such values are difficult to obtain from single crystal X-ray diffraction data. Hydrogen bond distances can be obtained from neutron diffraction data but such studies are rare.

Three low intensity Raman bands are observed at 2016, 2365 and 2704 cm^{-1}. The assignment of these bands is not known but one possible attribution is to the stretching mode of very strongly hydrogen bonded water. These bands using a Libowitzky type function [43] given above, give hydrogen bond distances of 2.550, 2.553 and 2.595 Å. The bands at 1767 and 1587 cm^{-1} may be ascribed to water HOH bending modes. Such bands are assigned to very strongly hydrogen bonded water molecules. The position of such bands harmonise well with the bands attributed to very strongly hydrogen bonded water.

CONCLUSIONS

Raman spectroscopy has been used to characterise the molecular structure of the mineral parnauite $Cu_9(AsO_4)_2(SO_4)(OH)_{10}\cdot 7H_2O$. Characteristic Raman bands of the $(AsO_4)^{3-}$ stretching and bending vibrations were identified and described. Raman bands attributable to the OH stretching vibrations of water and hydroxyl units were analysed. A comparison was made with the Raman spectrum of parnauite with other selected basic copper arsenate minerals.

Acknowledgments

The financial and infra-structure support of the Queensland University of Technology, Inorganic Materials Research Program is gratefully acknowledged. The Australian Research Council (ARC) is thanked for funding the instrumentation. This work was supported by Ministry of Culture of the Czech Republic (MK00002327201) to Jiří Sejkora.

REFERENCES

1. Lai L, Li Y, Shi N *Yanshi Kuang. Zazhi* **1997**, *16*, 50-55.
2. Sarp H, Deferne J, Liebich BW *Arch. Scienc.***1978**, *31*, 213-17.
3. Wise WS *Amer. Min.***1978**, *63*, 704-8.
4. Anthony JW, Bideaux RA, Bladh KW, Nichols MC *Handbook of Mineralogy*; Mineral Data Publishing: Tuscon, Arizona, USA, 2000; Vol. 4.
5. Frost RL, Cejka J, Ayoko G *J. Raman Spectrosc.* **2008**, *39*, 495-502.
6. Frost RL, Cejka J, Ayoko GA, Dickfos MJ *J. Raman Spectrosc.* **2008**, *39*, 374-379.
7. Frost RL, Cejka J, Dickfos MJ *J. Raman Spectrosc.* **2008**, *39*, 779-785.
8. Frost RL, Cejka J, Keeffe EC, Dickfos MJ *J. Raman Spectrosc.* **2008**, *39*, 1413-1418.
9. Frost RL, Dickfos MJ, Cejka J *J. Raman Spectrosc.* **2008**, *39*, 582-586.
10. Frost RL, Dickfos MJ, Cejka J *J. Raman Spectrosc.* **2008**, *39*, 1158-1161.
11. Frost RL, Dickfos MJ, Reddy BJ *J. Raman Spectrosc.* **2008**, *39*, 1250-1256.
12. Frost RL, Hales MC, Wain DL *J. Raman Spectrosc.* **2008**, *39*, 108-114.
13. Frost RL, Keeffe EC *J. Raman Spectrosc.* **2008**, *in press*.
14. Frost RL, Keeffe EC *J. Raman Spectrosc.* **2008**, *39*, 1408-1412.
15. Frost RL, Locke A, Martens WN *J. Raman Spectrosc.* **2008**, *39*, 901-908.
16. Frost RL, Reddy BJ, Dickfos MJ *J. Raman Spectrosc.* **2008**, *39*, 909-913.
17. Hales MC, Frost RL, Martens WN *J. Raman Spectrosc.* **2008**, *39*, 1141-1149.
18. Palmer SJ, Frost RL, Ayoko G, Nguyen T *J. Raman Spectrosc.* **2008**, *39*, 395-401.
19. Zhao Y, Frost RL *J. Raman Spectrosc.* **2008**, *39*, 1494-1501.
20. Zhao Y, Yang J, Frost RL *J. Raman Spectrosc.* **2008**, *39*, 1327-1331.
21. Vansant FK, Veken BJVd, Desseyn HO *J. Mol. Struct.* **1973**, *15*, 425-437.
22. Busey RH, Keller OL *J. Chem. Phys.* **1964**, *41*, 215-225.
23. Myneni SCB, Traina SJ, Waychunas GA, Logan TJ *Geochim. Cosmochim. Acta* **1998**, *62*, 3285-3300.
24. Ross SD In *The infared spectra of minerals* Farmer VC, Ed.; Mineralogical Society: London 1974.
25. Frost RL, Kloprogge JT *Neues Jahrb. Mineral., Monatsh.* **2001**, 27-40.
26. Martens W, Frost RL, Kloprogge JT, Williams PA *J. Raman Spectrosc.* **2003**, *34*, 145-151.
27. Martens WN, Kloprogge JT, Frost RL, Rintoul L *J. Raman Spectrosc.* **2004**, *35*, 208-216.
28. Frost RL, Martens W, Williams PA, Kloprogge JT *J. Raman Spectrosc.* **2003**, *34*, 751-759.
29. Martens W, Frost RL, Kloprogge JT *J. Raman Spectrosc.* **2003**, *34*, 90-95.
30. Martens W, Frost RL, Williams PA *J. Raman Spectrosc.* **2003**, *34*, 104-111.
31. Frost RL, Kloprogge JT, Martens WN *J. Raman Spectrosc.* **2004**, *35*, 28-35.
32. Frost RL, Martens WN, Williams PA *J. Raman Spectrosc.* **2002**, *33*, 475-484.
33. Frost RL, Williams PA, Martens W, Kloprogge JT *J. Raman Spectrosc.* **2002**, *33*, 752-757.
34. Sumin De Portilla VI *Can. Mineral.* **1974**, *12*, 262-8.
35. Farmer VC *Mineralogical Society Monograph 4: The Infrared Spectra of Minerals*, 1974.
36. Griffith WP *J. Chem. Soc.* **1970**, 286-91.
37. Huminicki DMC, Hawthorne FC *Rev. Min.* **2002**, *48*, 123-325.
38. Hawthorne FC *Zeit. Krist.* **1992**, *201*, 183-206.
39. Emsley J *Chem. Soc. Rev.* **1980**, *9*, 91-124.
40. Lutz H *Struct. Bond.* **1995**, *82*, 85-103.
41. Mikenda W *J. Mol. Struc.* **1986**, *147*, 1-15.

42. Novak A *Struct. Bond.* **1974**, *18*, 177-216.
43. Libowitzky E *Monatsh. Chem.* **1999**, *130*, 1047-1059.

List of Fig.s

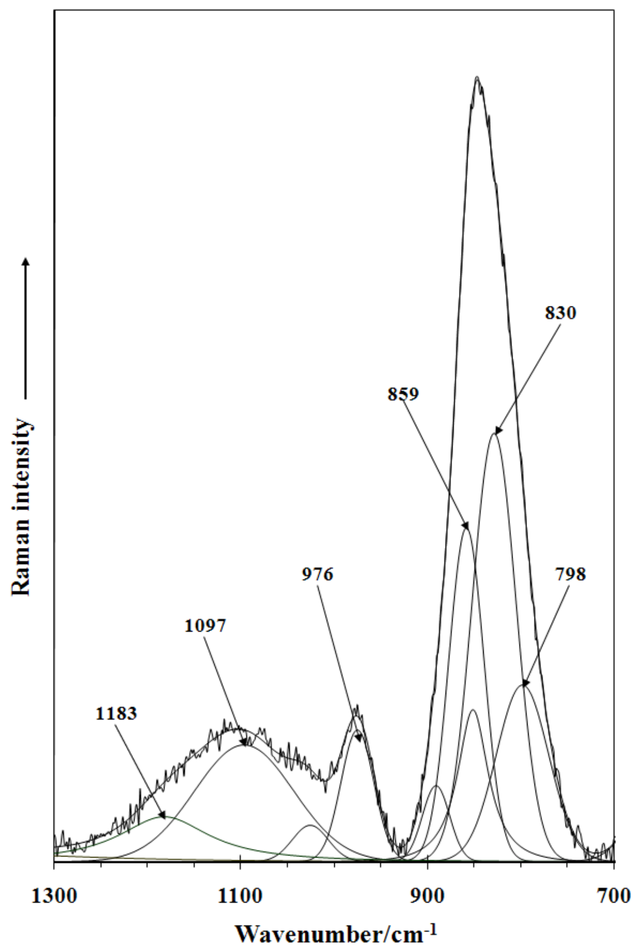

Raman intensity
1183
1097
976
859
830
798
1300
1100
900
700
Wavenumber/cm-1

Fig. 1

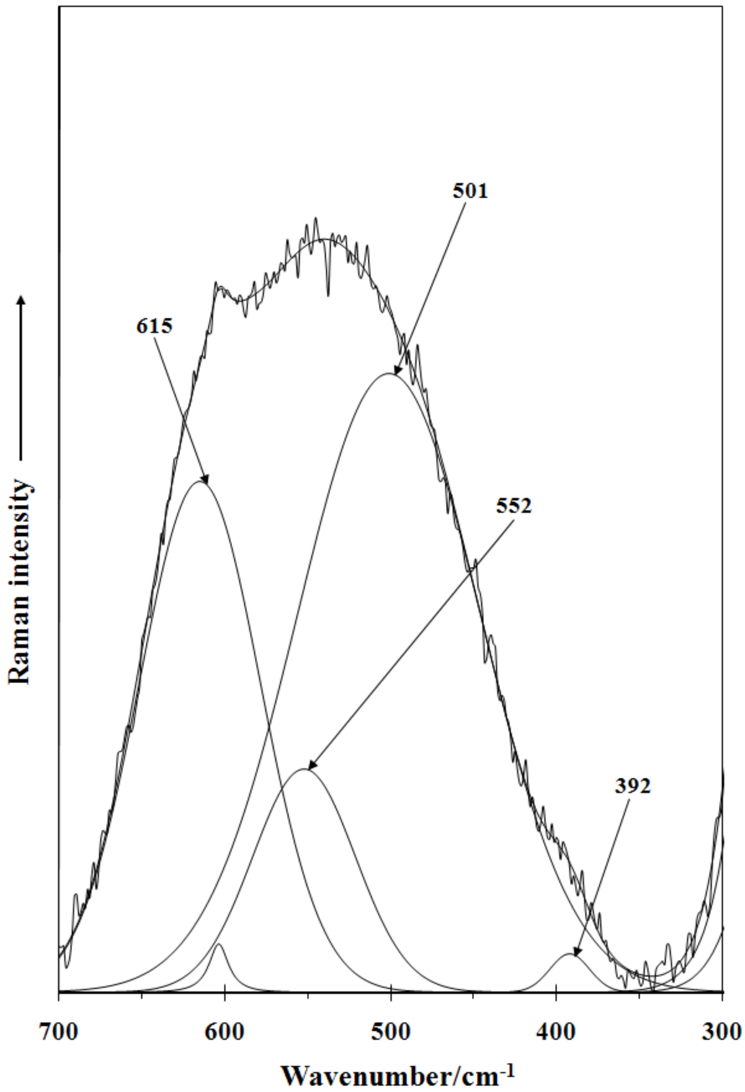
501
615
552
392
Raman intensity
700
600
500
400
300
Wavenumber/cm-1

Fig. 2

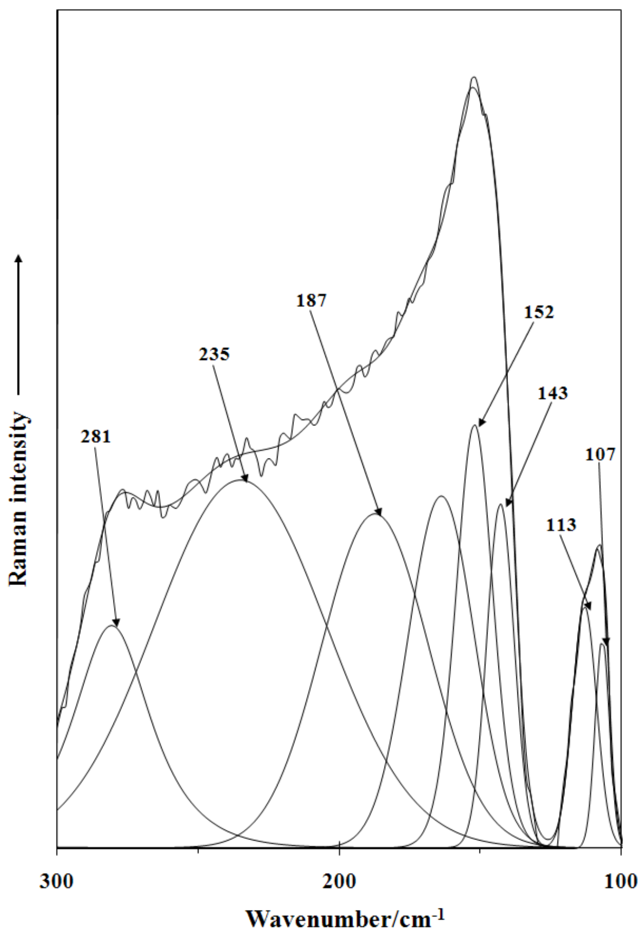

Raman intensity
281
235
187
152
143
107
113
300
200
100
Wavenumber/cm-1

Fig. 3

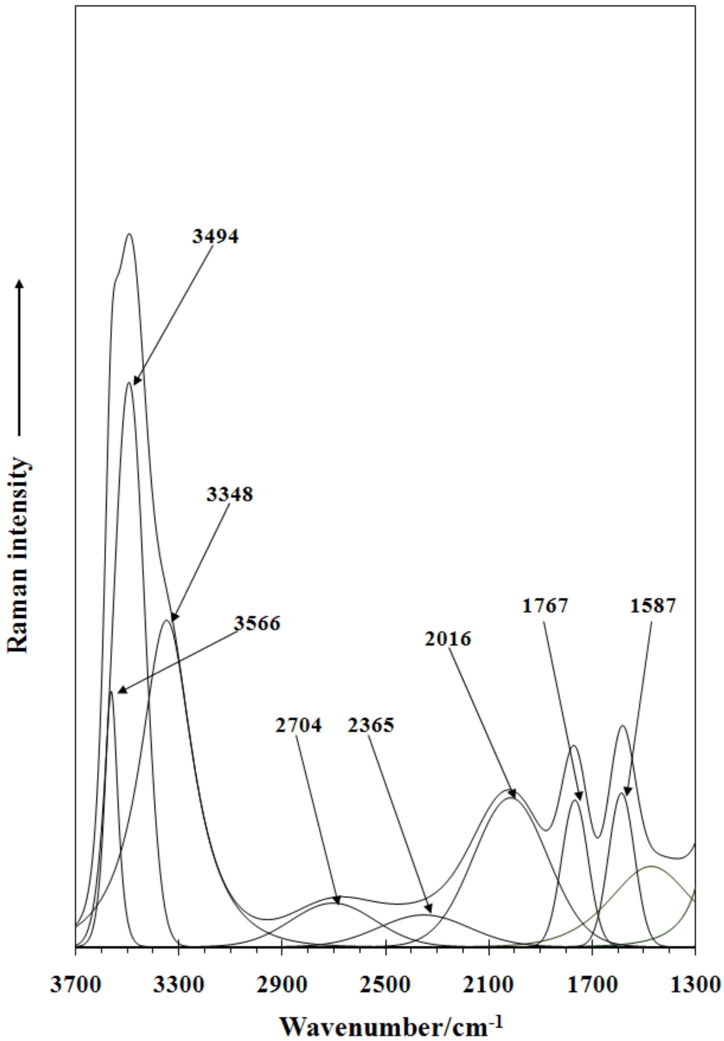
Raman intensity
3494
3348
3566
2704
2365
2016
1767
1587
3700
3300
2900
2500
2100
1700
1300
Wavenumber/cm-1

Fig. 4